# Heat Transfer Characteristics of Boiling Nitrogen and Neon in Narrow Annuli

**ABRAHAM LAPIN, H. C. TOTTEN, and L. A. WENZEL**

**Air Products and Chemicals, Inc., Allentown, Pennsylvania**

**The boiling characteristics of liquid neon and nitrogen in vertical annuli ranging between 0.006 and 0.080 in. wide were studied. The center tube wall, submerged to various depths, formed the boiling surface. Observations suggested a convective heat transfer mechanism, and correlation by a Dittus-Boelter equation form proved successful.**

Interest in cryogenically cooled magnets is rapidly increasing in view of the substantial energy reduction achieved at low temperatures. The compactness and low resistivity obtainable with cryomagnets are necessary to obtain very high field strengths in the order of $10^5$ oersteds or higher.

Magnets may be maintained at their desired temperatures by removing the required energy input as sensible heat in a fluid or as latent heat. Air, water, or kerosene are used for magnets operating at ambient temperatures. Removal of the heat generated in cryogenic magnets by means of a boiling liquid offers two major advantages over the use of a fluid utilizing sensible heat transfer: a lower temperature difference can be maintained between the boiling liquid and the magnet surface, hence, a lower resistivity, and a much smaller volume of coolant is required.

At 30°K. the only fluid refrigerants are helium, hydrogen, and neon. Hydrogen and neon are more suitable from the heat transfer point of view, but safety considerations preclude the use of liquid hydrogen until more operating experience with cryomagnets is obtained. Other refrigerants are available for operation at higher cryogenic tempeatures. Some cryogenically cooled magnets have been operated at 78°K. by using liquid nitrogen as a coolant.

The investigation was divided into two parts: 1. Study of pool boiling on a short vertical pipe with liquid nitrogen and neon. 2. Study of nitrogen and neon boiling in narrow annuli.

The first part of this study was presented at the A.I.Ch.E. National Meeting, Pittsburgh, Pennsylvania (*1*). This paper will present the second part of the study covering the various factors affecting the boiling performance in narrow annuli.

The technical literature contains many studies and analyses of heat transfer to boiling liquids. These studies take many forms such as surveys (*2, 3*), theoretical analyses (*4, 5, 6, 7, 8*), experimental work (*9, 10, 11, 12*), and statistical analyses (*13, 14*). Heat transfer to boiling cryogenic liquids has been thoroughly reviewed by Class et al. (*2*) and Richards et al. (*3*). Both conclude that there are large variations in the magnitude of heat flux and in the shape of the heat flux vs. temperature difference curves, obtained by different investigators. These differences may be due to uncontrolled parameters such as surface roughness and contamination.

The study of heat transfer to boiling liquids flowing in narrow channels is limited. The following is a brief review of the pertinent literature in this area.

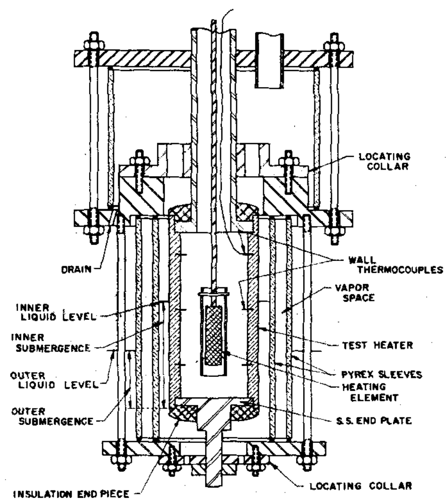


**Fig. 1. Sketch of assembled test section.**

Neusen, Kangas, and Sher (*15*) studied heat transfer and pressure drop for superheated steam flowing in thin annular passages at 600 lb./sq.in.abs. The test section consisted of annuli formed by an 0.878-in. O.D. tube inside of an 0.997-in. I.D. tube, giving a gap of 0.0595 in. The authors determined that the Heineman's correlation of Nusselt number for $L/De$ greater than 60 correlated their data for superheated steam in the thin annulus with both walls heated. Heineman derived the following correlation

$$(N_{Nu})_f = 0.0133\,(N_{Re})_f^{0.84}\,(N_{Pr})_f^{1/3} \text{ for } L/De \geqq 60 \tag{1}$$

when short round tubes and rectangular channels having an equivalent diameter of 0.332 and 0.091 in., respectively, were investigated at high pressures and temperatures.

Polomik, Levy, and Sawochka (*16*) investigated the heat transfer coefficients at elevated pressures for annular flow with water boiling to 100% quality. The study was made in an 0.625-in. O.D. tube with two annuli 0.060 and 0.120 in. The surface finish of their stainless steel surface was 50 $\mu$in. or better. The experimental data were correlated within ± 20% by using a Colburn type of equation modified by steam quality and steam void groupings. The correlation applied only to the film boiling data. The authors, however, discussed the three boiling regions: nucleate boiling, transition region, and film boiling region. The data obtained in the nucleate boiling region and transition zone were tabulated, but not correlated, in their paper.

L. A. Wenzel is at Lehigh University, Allentown, Pennsylvania.

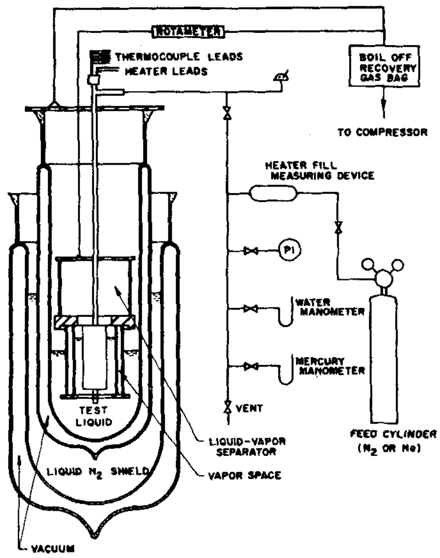


**Fig. 2. Schematic diagram of test section.**

Kapinos and Nikitenko (*17*) correlated the data obtained in their study of heat transfer in channels by means of an equation of the type $N_{Nu} = f(N_{Re})$. They modified the characteristic length of both the Nusselt and Reynolds number by the introduction of a size factor correction.

Only two references related to the investigation of cryogenic fluids boiling in narrow passages were found. The first one by Sydoriak and Roberts (*18*) determined experimentally the critical heat input to liquid hydrogen and nitrogen boiling in an annular gap. They derived the following equation

$$Q = AL\ (\rho_{v2}\,\rho_L\,Z_e\,g\,f_2)^{1/2} \tag{2}$$

on the assumption of a homogeneous and frictionless two-phase flow. The second one by Richards, Robbins, Jacobs, and Holten (*19*) duplicated Sydoriak's work. The heat transfer test section which was identical to the one used by Sydoriak and Roberts simulated the design of an electromagnet operable at a low temperature of 20°K. It consisted of a 7 in. long stainless steel plug which was accurately centered in a 5 in. long stainless steel tube. Various sizes of plugs were used in order to obtain different size annular spaces in the test section. Gap sizes between 7 and 20 mils were tested. The authors concluded that a prediction of the maximum operating power of an electromagnet by theoretical analysis is not reliable at this time.

## EXPERIMENTAL PROGRAM

### Test Section and Instrumentation

A complete description of the principles involved in the test section design as well as of the basic test section and its instrumentation has been made previously (*1, 20*).

TABLE 2. PROPERTIES OF NITROGEN AND NEON

| Liquid at boiling point | Nitrogen (*21*) | Neon |
|---|---|---|
| Viscosity, lb./ft.-hr. | 0.385 | 0.714 (*23, 24*) |
| Thermal conductivity, lb./hr.-ft.-°F. | 0.0805 | 0.0752 (*25*) |
| Surface tension, lb./ft. | 0.0006 | 0.00032 (*21*) |
| Specific heat, B.t.u./lb.-°F. | 0.476 | 0.427 (*21*) |
| Latent heat, B.t.u./lb.-mole | 2405 | 748 (*21*) |
| **Vapor at boiling point** | | |
| Density, lb./cu. ft. | 0.2939 | 0.56 (*21*) |
| Viscosity, lb./ft.-hr. | 0.012 | 0.0124 (*26*) |
| Thermal conductivity, lb./hr.-ft.-°F. | 0.0043 | 0.0236 (*21*) |
| Heat capacity, B.t.u./lb.-°F. | 0.20 | 0.44 (*21*) |

Figures 1 and 2 show the details and the assembly of the test heater and the flow sheet of the complete experimental section. The only difference between the test heater used for the narrow annuli study and the one used for pool boiling is the addition of the precision Pyrex sleeve and the related hardware as shown in Figure 1.

An important consideration was the determination of the exact gap size at the liquid nitrogen and neon temperatures. This was accomplished by accurate measurements of the outside diameter of the heater and the inside diameter of the precision Pyrex sleeve at ambient temperature. The best available coefficients of thermal expansion as a function of temperature for the OFHC (oxygen free high conductivity) copper and the Pyrex sleeve (*21, 22*) were used to calculate the contraction of both materials from ambient to liquid nitrogen and neon temperatures. Detailed calculations show that a differential contraction of 0.004 in. occurs between the copper and Pyrex for both the liquid nitrogen and neon cases. The gap dimension at liquid nitrogen and neon temperature is therefore the gap size measured at ambient conditions plus the differential contraction correction of 0.004 in.

Since the tests are to be carried out at cryogenic temperatures, heat leak to the test section is an important factor. Calculations show that the precision glass sleeve offers sufficient resistance to render the heat leak effect negligible. However, it was decided to minimize this effect further by the addition of a second Pyrex pipe around the precision Pyrex pipe, thus forming a vapor barrier.

### Experimental Procedure

The experimental procedure consisted of assembling the test section and introducing it to the glass dewars assembly shown in Figure 2. The heater cavity was evacuated, and the whole section was then cooled with either liquid nitrogen or neon. The shield section of the dewars assembly was filled with liquid nitrogen. Gaseous nitrogen or neon, depending on which fluid was being investigated, was introduced in the 500-cc. heater cavity until half of it was filled with liquid.

Four major gap sizes were tested, namely, 6, 20, 53, and 80 mils, at liquid nitrogen and neon temperatures. Two additional gap widths of 21 and 22 mils were also tested in the case of the nickel plated and cadmium plated heaters, respectively. Two submergences were considered: the inner submergence defined as the length of the heater surface which

TABLE 1. CHARACTERISTIC DIMENSIONS OF TEST SECTIONS

| Heater No. | Heater O.D.-in., $D_1$ | Glass sleeve I.D.-in., $D_2$ | Gap size at liq. Ne & $N_2$ temp., in., $t$ | Annular flow area sq. ft., $A_t$ | Equivalent diameter in., $De$ | Heat transfer area, sq. ft./in. | Surface finish RMS, $\mu$ in. |
|---|---|---|---|---|---|---|---|
| 12*b* | 2.9975 | 3.0015 | 0.006 | $3.916 \times 10^{-4}$ | 0.024 | 0.06540 | 9-11 (Cu) |
| 6 | 2.9695 | 3.0015 | 0.020 | $13.01 \times 10^{-4}$ | 0.080 | 0.06478 | 16-20 (Cu) |
| 9 | 2.9675 | 3.0015 | 0.021 | $13.65 \times 10^{-4}$ | 0.084 | 0.06474 | 6-8 (Ni) |
| 10 | 2.9645 | 3.0015 | 0.022 | $14.12 \times 10^{-4}$ | 0.088 | 0.06468 | 8-11 (Cd) |
| 7*b* | 2.9030 | 3.0015 | 0.053 | $34.09 \times 10^{-4}$ | 0.212 | 0.06333 | 11-13 (Cu) |
| 8 | 2.8495 | 3.0015 | 0.080 | $50.99 \times 10^{-4}$ | 0.320 | 0.06217 | 13-15 (Cu) |

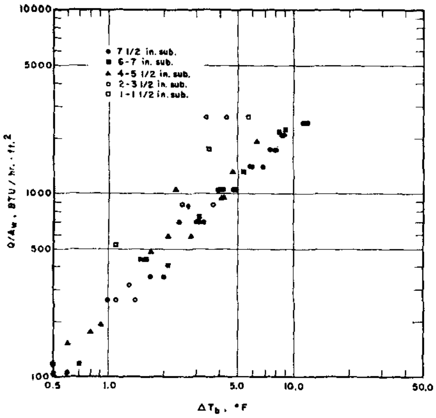


**Fig. 3. Heat flux vs. temperature driving force ($\Delta T_b = T_w - T_{sat}$), nitrogen annular gap boiling, copper heater, 6-gap dimension at liquid nitrogen temperature 20 mils.**

is wetted by the boiling liquid and the outer submergence defined as the depth of the lower edge of the heater relative to the liquid level outside the annulus. Both submergences are identified in Figure 1.

A series of runs for annular gap boiling consisted of varying the electric power input to the electric element at at least two inner submergences. Heater pressure, wattage, wall temperatures, and both inner and outer submergences were measured for each run.

The characteristic dimensions of the six test heaters are summarized in Table 1. All these six heaters were previously tested under pool boiling conditions. The physical properties of the two cryogenic fluids tested, nitrogen and neon, which are not easily available in the literature, are listed in Table 2.

### Experimental Results and Observations

All the experimental data were reduced to the form of heat flux as a function of temperature driving force.

The nitrogen data for the 20 mil gap heater plotted in Figure 3 represent a typical condition and show the effect of submergence on heat flux. All the data taken with a 7½-in. submergence for nitrogen and neon are plotted in Figures 4 and 5, respectively.

Observation of the annular gap boiling showed the existence of a convective type of heat transfer disturbed by bubbles rising to the surface. Actually, the heater surface was completely covered by a layer of liquid which was interrupted only at the bubble sites. Furthermore, it was noted that the actual bubble site area was a small fraction of the total heating area. It appeared that the only effect of the rising bubbles was to increase the turbulence of the liquid flowing in the annulus.

### Treatment of Data

In view of these observations, it is reasonable to treat the annular gap boiling case in a manner similar to the one used for convective heat transfer. This approach was used by other investigators (*27, 15, 16*) and was the starting point of most theoretical derivations (*28, 29, 7*). However, factors affecting bubble formation and behavior should also be considered.

The following generalized equation incorporating all factors affecting boiling, bubble formation, and bubble behavior is obtained by dimensional analysis:

$$\frac{h_b D}{k_L} = a'\left(\frac{DG}{\mu_L}\right)^b \left(\frac{L}{D}\right)^c \left(\frac{Cp_L \mu_L}{k_L}\right)^d \left(\frac{\mu_L^2}{\rho_L g_c D \sigma}\right)^e \times \left(\frac{\mu_L^2}{\rho_L g_c D^2 P_V}\right)^f \left(\frac{\rho_L}{\rho_v} - 1\right)^g \quad (3)$$

Liquid properties for thermal conductivity, density, and heat capacity are used, since it was experimentally observed that heat is transferred through a liquid film.

The present experimental work covering only nitrogen and neon does not permit determination of the exponents for all the terms of Equation (3). A simplification of this equation will result in

$$\frac{h_b De}{k_L} = a\left(\frac{De\,G}{\mu_L}\right)^b \left(\frac{L}{De}\right)^c \left(\frac{Cp_L \mu_L}{k_L}\right)^d \quad (4)$$

where $De$ is the conventional equivalent diameter defined as (4 × flow area)/(wetted perimeter). This equation includes the most important properties affecting heat transfer, as well as the characteristic dimensions of the annular gap. The coefficient and exponents of this equation can now be obtained from the experimental data obtained in this work.

The coefficient and exponents for Equation (4) were obtained by the method of least squares with a GE-225 computer, resulting in

$$(N_{Nu})_L = 150\ (N_{Re})_L^{0.18}\ (L/De)^{-0.82}\ (N_{Pr})_L^{0.96} \quad (5)$$

which represents all the experimental data, nitrogen, and neon, with an average percent deviation of ± 23%. The measured Nusselt numbers are compared with the calculated ones in Figure 6.

Equations for each individual heater can be easily calculated. For example, equations for annular gap nitrogen boiling at full submergence are

$$(N_{Nu})_L = 17.3\ (N_{Re})_L^{0.18} \text{ for 0.053-in. gap} \quad (6)$$

and

$$(N_{Nu})_L = 24.4\ (N_{Re})_L^{0.18} \text{ for 0.080-in. gap} \quad (7)$$

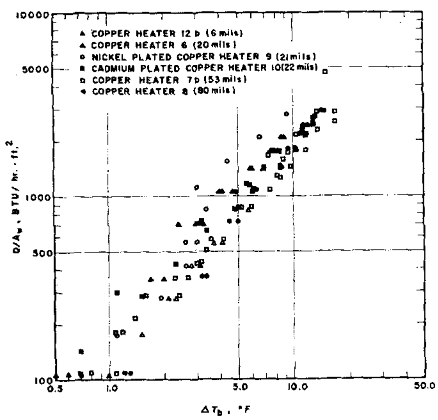


**Fig. 4. Heat flux vs. temperature driving force ($\Delta T_b = T_w - T_{sat}$), nitrogen annular gap boiling, comparison between all heaters at 7½ in. inner submergence.**

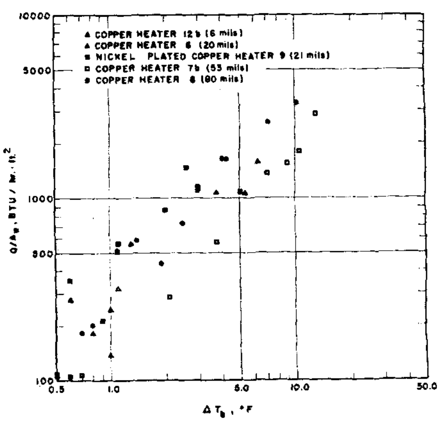


**Fig. 5. Heat flux vs. temperature driving force ($\Delta T_b = T_w - T_{sat}$), neon annular gap boiling, comparison between all heaters at 7½ in. inner submergence.**

These equations are shown in Figures 7 and 8, respectively.

The agreement between the correlation and the experimental data is noteworthy in view of the wide range of experimental conditions. The following discussion briefly reviews the effect of the important experimental conditions on the boiling coefficients.

*Surface Roughness and Finish.* The measured root mean square roughness and surface finish appear to have no effect on boiling coefficients in annular gap boiling, at least within the limits of this work. This apparent independence of annular gap boiling from surface effect has also been observed with respect to surface oxidation. Two runs were made with a copper heater having about 15% of its surface badly oxidized. These runs were repeated with the heater surface completely cleaned, and the coefficients calculated from the new data were the same as the ones calculated from the old data.

*Effect of Back Pressure on Boiling.* Several runs were performed with the rotameter line connected to the vapor liquid separator as shown in Figure 2. The effect of the back pressure created by the rotameter on the system was very noticeable. The liquid level inside the annulus was immediately lowered to a point about 1 in. below the outer liquid level. The appearance of the foam was also changed. Its height was reduced from 1 in. or so to about ¼ in. or less. Entrainment, if any, was completely stopped. Vapor bubbles appear to become smaller. All in all, the back pressure effect on the nature of the gap boiling was significant.

However, in spite of the different appearance of boiling, the heat transfer coefficients calculated for the cases of connected and unconnected rotameter were the same.

*Effect of Entrainment.* Entrainment occurred when the combination of heat input and outer submergence was sufficient to raise liquid droplets into the entrainment collector. Examination of data taken with and without entrainment shows that at a given heat flux the boiling temperature driving force is slightly smaller for the case having entrainment. This is caused by the larger flow existing in the annulus during entrainment resulting in a better performance. The effect, however, was usually small. Differences in temperature driving forces were usually of the order of 0.2 to 0.4°F. at the higher heat fluxes, or the equivalent of 2 to 3% of the temperature driving force.

*Comparison Between Neon and Nitrogen Boiling.* There were no apparent differences between neon and nitrogen boiling in narrow annuli. Data, however, showed that at a given temperature difference, heat flux for neon was higher than for nitrogen. This can be seen by comparing Figures 4 and 5.

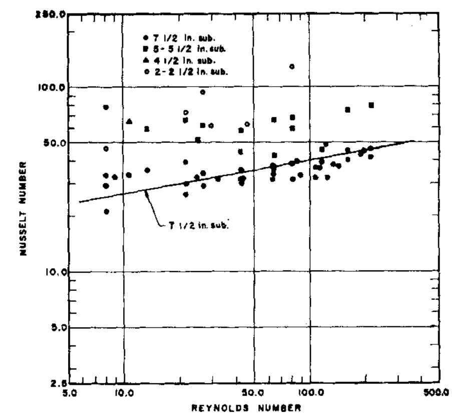


Fig. 7. Nusselt number vs. Reynolds number, nitrogen annular gap boiling, copper heater 7b, 53-mil gap.

*Maximum Heat Flux.* Maximum heat fluxes due to gap size were experienced in four cases only:

1. 850 B.t.u./hr.-sq.ft. at $\Delta T_b$ = 5.8°F. for liquid nitrogen in a 6-mil gap heater.
2. 350 B.t.u./hr.-sq.ft. at $\Delta T_b$ = 1.1°F. for liquid neon in a 6-mil gap heater.
3. 1,600 B.t.u./hr.-sq.ft. at $\Delta T_b$ = 6.5°F. for liquid neon in a 20-mil gap heater.
4. 1,600 B.t.u./hr.-sq.ft. at $\Delta T_b$ = 3.0°F. for liquid neon in a 21-mil gap heater.

In all other cases, limit on heat flux was the result of heat input limitation rather than gap size effect.

*Evaluation of the Sydoriak and Roberts Correlation.* The ratio of heat fluxes calculated by means of the Sydoriak and Roberts equation [Equation (2)] to measured ones varies between 1.2 and 2.2 for nitrogen boiling in annuli having 20- to 22-mil gap sizes. This ratio is 5.4 and 6.9 for nitrogen boiling in annuli having a gap size of 53 and 80 mils, respectively. It is therefore apparent that the Sydoriak and Roberts equation does not apply to gap sizes larger than 22 mils.

## CONCLUSIONS

An investigation of neon and nitrogen boiling in narrow annuli was completed. The study covered the case of a 7½ in. long vertical heater with a nominal 3-in. O.D., gap sizes ranging from 0.006 to 0.080 in., and $L/De$ ratios varying between 9 and 310.

The experimental design concept allowed for visual observation simultaneously with data collection, which

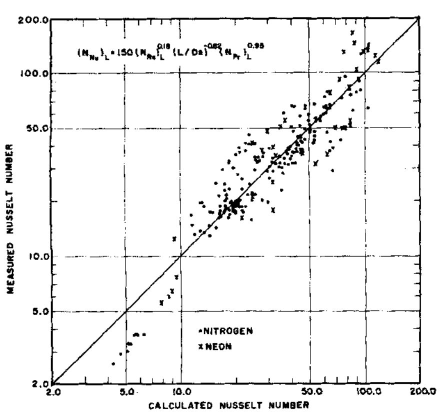


Fig. 6. Comparison between measured and calculated Nusselt number for all neon and nitrogen annular flow boiling data.

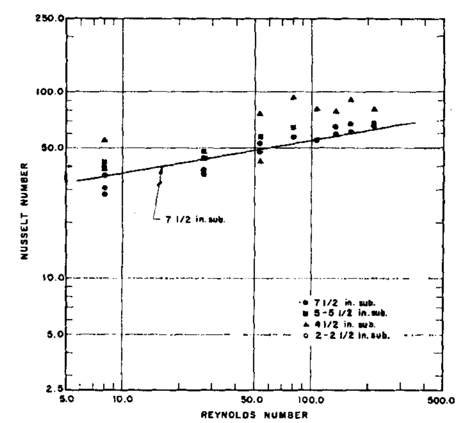


Fig. 8. Nusselt number vs. Reynolds number, nitrogen annular gap boiling, copper heater 8, 80-mil gap.

made it possible to relate data directly to observed behavior.

A generalized equation for annular gap boiling was derived on the assumption of convective type of heat transfer. The concept of equivalent diameter was used to modify the characteristic dimension in the Nusselt and Reynolds numbers.

The following equation correlated all annular gap boiling data obtained with nitrogen and neon with an average percent deviation of ± 23%:

$$\frac{h_b De}{k_L} = 150 \left(\frac{De\,G}{\mu_L}\right)^{0.18} \left(\frac{L}{De}\right)^{-0.82} \left(\frac{Cp_L\,\mu_L}{k_L}\right)^{0.96} \tag{8}$$

The validity of the correlation over the wide range of parameters involved in the experimental work substantiates the assumptions made and concepts involved in the derivation of the equation.

However, caution should be exercised in the use of Equation (8) outside the range of the experimental work. It is believed that while this equation would be satisfactory for cryogenic fluids in general, certain size limitations should be considered, namely vertical height less than 15 in. and annular gap sizes in the order of 0.006 to 0.080 in. It should be noted, however, that this range of gap sizes effectively covers the practical range for narrow annuli. The lower limit of 0.006 in. is very nearly a practical minimum. A gap size exceeding the upper limit of 0.080 in. will result in a condition equivalent to pool boiling.

## ACKNOWLEDGMENT

This study was performed at Air Products and Chemicals, Inc., under NASA Contract No. NASr-107 and was part of the Doctoral Dissertation presented by A. Lapin to the Graduate Faculty of Lehigh University in 1963.

The authors wish to acknowledge the efforts and contribution of Drs. J. M. Geist and Clyde McKinley and wish to thank APCI and NASA for their permission to publish.

## NOTATION

$a, a'$ = constants
$A$ = cross-sectional area of annular gap, sq.ft.
$A_t$ = test section annular flow area, sq.ft.
$A_w$ = test section wetted effective heat transfer area, sq.ft.
$b$ = constant
$c$ = constant
$Cp_f$ = heat capacity at film conditions, B.t.u./(lb.)(°F.)
$Cp_L$ = heat capacity of liquid, B.t.u./(lb.)(°F.)
$d$ = constant
$D$ = diameter, ft.
$De$ = equivalent diameter = $\frac{4 \text{ flow area}}{\text{wetted perimeter}}$, ft.
$D_1$ = outside diameter of heater, in.
$D_2$ = inside diameter of glass sleeve, in.
$e$ = constant
$f$ = constant
$f_2$ = mass fraction vapor in the fluid leaving heater
$g$ = constant
$g$ = acceleration of gravity, 32.2 ft./sec.$^2$
$g_c$ = conversion factor from force to mass
$G$ = mass flow velocity, lb./(hr.)(sq.ft.)
$h_b$ = boiling heat transfer coefficient, B.t.u./(hr.)(sq.ft.)(°F.)
$k_f$ = thermal conductivity at film conditions, B.t.u./(hr.)(ft.)(°F.)
$k_L$ = thermal conductivity of liquid, B.t.u./(hr.)(ft.)(°F.)
$L$ = wetted length of surface, ft.
$(N_{Nu})_f$ = Nusselt number at film conditions = $\frac{h_b De}{k_f}$, dimensionless
$(N_{Nu})_L$ = Nusselt number based on liquid properties = $\frac{h_b De}{k_L}$, dimensionless
$(N_{Pr})_f$ = Prandtl number at film conditions = $\frac{Cp_f \mu_f}{k_f}$, dimensionless
$(N_{Pr})_L$ = Prandtl number based on liquid properties = $\frac{Cp_L \mu_L}{k_L}$, dimensionless
$(N_{Re})_f$ = Reynolds number at film conditions = $\frac{De\,G}{\mu_f}$, dimensionless
$(N_{Re})_L$ = Reynolds number based on liquid properties = $\frac{De\,G}{\mu_L}$, dimensionless
$P_V$ = liquid vapor pressure
$Q$ = heat transfer rate, B.t.u./sec. [Equation (2)]
$Q$ = heat transfer rate, B.t.u./hr. (Figures 3, 4, 5)
$t$ = test section gap size at liquid nitrogen and neon temperatures, in.
$T_{sat}$ = saturation temperature, °F.
$T_w$ = temperature of heating surface, °F.
$Z_e$ = hydrostatic head, ft.
$\Delta T_b$ = boiling temperature driving force = $T_w - T_{sat}$, °F.
$\mu_f$ = viscosity at film conditions, lb./(ft.)(hr.)
$\mu_L$ = viscosity of liquid, lb./(ft.)(hr.)
$\rho_L$ = density of liquid, lb./cu.ft.
$\rho_V$ = density of vapor, lb./cu.ft.
$\rho_{V2}$ = exit vapor density, lb./cu.ft.
$\sigma$ = surface tension, lb./ft.

## LITERATURE CITED

1. Lapin, A., H. C. Totten, and L. A. Wenzel, *A.I.Ch.E. J.*, **11**, No. 2, p. 197 (1965).
2. Class, C. R., J. R. DeHaan, M. Piccone, and R. B. Cost, *Beechcraft R & D Engineering Report No. 6154* (October, 1958).
3. Richards, R. J., W. G. Steward, and R. B. Jacobs, *N. B. S. TN 122 PB 161623*, Bureau of Standards, Washington, D. C. (October, 1961).
4. Zuber, N., *Int. J. Heat Mass Transfer*, **6**, 53-78 (1963).
5. ———, and E. Fried, "Two-Phase Flow and Boiling Heat Transfer to Cryogenic Liquids," pp. 1709-61, ARS—Propellants, Combustion and Liquid Rockets Conference, Palm Beach, Florida (April 26-28, 1961).
6. ———, *ARS Journal*, **32**, 1332-1341 (September, 1962).
7. Rohsenow, W. M., *Trans. Am. Inst. Mech. Engrs.*, **74**, 338-352, 969-996 (1952).
8. ———, "Heat Transfer Symposium Series," p. 1011, Univ. Mich., Ann Arbor, Michigan (1952).
9. Drayer, D. E., and K. D. Timmerhaus, "Advances in Cryogenic Engineering," K. D. Timmerhaus, ed., Vol. 7, Plenum Press, New York (1962).
10. Haselden, G. C., and J. I. Peters, *Trans. Inst. Chem. Engrs.*, London, **27**, (1949).
11. Weil, L., and A. Lacaze, *Compt. Rend.*, **230-186** (1950).
12. ———, *J. Phys. Rad.*, **12**, 890 (1951).
13. Gaertner, R. F., *Chem. Eng. Progr. Symposium Ser. No. 41*, **59** 52-61.
14. Hughmark, G. A., *Int. J. Heat Transfer*, **5**, 667-672 (1962).
15. Neusen, K. F., G. J. Kangas, and N. C. Sher, *Chem. Eng. Progr. Symposium Ser. No. 41*, **59**, 185-192.

16. Polomik, E. E., S. Levy, and S. G. Sawochka, "Heat Transfer Coefficients with Annular Flow During 'One-Through' Boiling of Water to 100% Quality at 800, 1100 and 1400 Psi," GEAP-3703, Atomic Power Equipment Dept., G. E. Co., San Jose, California (May, 1961).
17. Kapinos, V. M., and N. I. Nikitenko, *Int. J. Heat Mass Transfer*, **6**, 271-276 (1963).
18. Sydoriak, S. G., and T. R. Roberts, *J. Appl. Phys.*, **28**, No. 2, pp. 143-148 (February, 1957).
19. Richards, R. J., R. F. Robbins, R. B. Jacobs, and D. C. Holten, "Advances in Cryogenic Engineering," K. D. Timmerhaus, ed., Vol. 3, pp. 375-89, Plenum Press, New York (1960).
20. Lapin, A., Ph.D. thesis, Lehigh University, Bethlehem, Pennsylvania (1963).
21. Air Products and Chemicals, Inc., Allentown, Pennsylvania, "Technical Data Book."
22. Johnson, V. J., U.S. Dept. of Commerce, *N.B.S. WADD Tech. Rept. 60-56 Part II* (October, 1960).
23. Cini-Castagnoli, G., G. Pizzella, and F. P. Ricci, *il Nuovo Cimento*, **11**, No. 3, pp. 466-467 (1954).
24. Hirschfelder, J. O., C. F. Curtis, and R. B. Bird, "Molecular Theory of Gases and Liquids," Wiley, New York (1954).
25. Cook, G. A., "Argon, Helium and the Rare Gases, I," Interscience, New York (1961).
26. Johnson, V. J., *N.B.S. WADD Rept. 60-56*, Part I (October, 1960).
27. McNelly, M. J., *J. Imp. Coll. Chem. Eng. Soc.*, **7**, 18-34 (1953).
28. Chen, J. C., ASME Paper No. 63-HT-34, Sixth National Heat Transfer Meeting, AIChE-ASME, Boston, August 11-14, 1963.
29. Guter, M., *Trans, Inst. Chem. Engrs.*, **29**, (1949).

*Manuscript received October 15, 1964; revision received December 9, 1964; paper accepted December 16, 1964. Paper presented at A.I.Ch.E. Boston meeting.*

# Determination of the Activity Coefficient of a Volatile Component in a Binary System by Gas-Liquid Chromatography

**CHUN F. CHUEH and WALDEMAR T. ZIEGLER**

**Georgia Institute of Technology, Atlanta, Georgia**

**The gas-liquid chromatographic (GLC) method of measuring the activity coefficient of the solute in a binary system has been extended from infinite dilution to the finite concentration range. An equation is presented relating the retention volume of the injected solute sample to the equilibrium solute concentration present in the column. This relation permits determination of the activity coefficient of the solute. Based on the experimental results obtained from the study of the two binary systems, benzene in diethylene glycol at 50°, 70°, and 90°C. and *n*-hexane in 1,2,4-trichlorobenzene at 30°C., the activity coefficients of the solute measured by the GLC method were found to agree within about ±5% with those obtained by the static equilibrium method.**

The vapor-liquid equilibrium of a volatile solute in a relatively nonvolatile solvent is difficult to measure by the conventional static equilibrium method because of the low equilibrium concentration of the solvent in the vapor phase and similarly the low concentration of the solute in the liquid phase. A number of investigators (*1, 4, 5, 9, 11, 13, 17*) have measured the activity coefficient of a solute at infinite dilution in such a nonvolatile solvent by the gas-liquid chromatographic (GLC) method. In this method the time required for a small solute sample to be carried through the column by an insoluble carrier gas, such as helium, is measured. The vapor-liquid equilibrium constant $K$ and hence the activity coefficient may be calculated from the retention volume by the equation

$$V_N = \overline{V}_G + \frac{1}{K}\left(\frac{\rho_L}{\rho_G}\right)\overline{V}_L \qquad (1)$$

The derivation of Equation (1) by Martin and Synge (*12*) and others (*9, 10, 15*) is based on the plate model and includes the assumptions that the sample size injected is small and no solute vapor is present in the insoluble carrier gas prior to the injection of the solute. The activity coefficient measured by this method is the activity coefficient of the solute at infinite dilution.

The object of the present study was to extend the GLC method for measuring the activity coefficient of the solute in a binary system from infinite dilution through a measurable concentration range. To accomplish this, a gaseous mixture of solute vapor and helium gas, instead of pure helium (or other inert gas), was used as the carrier gas. After the column had been flushed by the gaseous mixture for a sufficient length of time, the nonvolatile solvent inside the column became saturated with the solute, and hence an equilibrium state between the vapor phase and liquid phase was reached. Both phases contained a finite amount of solute. A small sample of the solute was then injected into the carrier gas entering the column, and its retention time was measured. The activity coefficient was calculated from the apparent retention time from the theoretical model presented below. By varying the concentration of the solute in the carrier gas, activity coefficients at various concentrations of the binary solution were determined. The experimental results have been compared with activity coefficient measurements obtained by others from vapor-liquid equilibrium measurements.

Chun F. Chueh is with Scientific Design Company, New York, New York.